Proceedings World Geothermal Congress 2000
Kyushu - Tohoku, Japan, May 28 - June 10, 2000

PERMEABLE FRACTURES AND IN-SITU STRESS AT THE KAKKONDA GEOTHERMAL FIELD, JAPAN

Osamu Kato[1], Takashi Okabe[2], Satoshi Shigehara[1], Nobuo Doi[1], Toshiyuki Tosha[3] and Kazuo Koide[3]

[1]Japan Metals & Chemicals Co., Ltd. (JMC), 72 Ukai, Takizawa-mura, Iwate, 020-0172, Japan
[2]Geothermal Energy Research and Development Co., Ltd. (GERD), 11-7, Kabuto-cho, Nihonbashi, Chuo-ku Tokyo, 103-0026, Japan
[3]New Energy and Industrial Technology Development Organization (NEDO)
3-1-1, Higashi-ikebukuro, Toshima-ku, Tokyo, 170-6028, Japan.

Key Words: fractures, stress, core, micro-earthquake, oxygen isotopes, Kakkonda geothermal field

ABSTRACT

Fourteen spot cores, many logs and micro-earthquake study reveal the fracture distribution and stress orientation around NEDO's well WD-1 continuously at northwest Kakkonda. This field has many fractures between the surface and ~3000m with various strikes and dips. The $\delta^{18}O$ value of the rock crystals within veins indicates whether the fracture is permeable or not. The permeable zone corresponds with the distribution of the open fractures independently of the fracture density. These fractures have been formed recently and some time ago. The permeable fractures are not necessarily formed in in-situ stress conditions at the present time. Permeable fractures formed some time ago keep opening and/or re-open under present stress conditions.

1. INTRODUCTION

The "Deep-seated Geothermal Resources Survey" project has been performed by New Energy and Industry Technology Development Organization (NEDO) in order to foster development of deep geothermal resources, which exist beneath already-developed shallow reservoirs. Well WD-1 at Kakkonda (depth; 1989m) was drilled in 1994-1995. WD-1a (depth; 3729m) was sidetracked at 1685m from WD-1. WD-1b (depth; 2963m) was sidetracked at 2193.5m from WD-1a in 1996-1997 (Fig. 1). WD-1 is the generic name for WD-1, WD-1a, and WD-1b in this paper.

By studying oriented and reoriented spot cores, and Schlumberger FMI logs from well WD-1, micro-earthquake data, and oxygen isotopic ratios, we have been able to determine, not only the types and distributions of reservoir fractures, but also their geometry and relative contributions to thermal-fluid flow at northwestern Kakkonda.

2. GEOLOGICAL SETTING

The Kakkonda geothermal field is hosted by a complex sequence of pre-Tertiary to Quaternary sedimentary and volcanic rocks (Kato et al., 1998). The pre-Tertiary to Tertiary rock sequence is disrupted by folds whose axes trend NW to NNW, and by major faults that trend NNW and E at late Miocene to Pleistocene (Fig. 1). These rocks have been intruded and metamorphosed by the 0.07-0.34 Ma Kakkonda Granite (Doi et al., 1998). Pre-Tertiary formations consist of slate, sandstone, and andesitic tuff (Fig. 2). Miocene formations of andesitic tuff, dacitic tuff, shale, and siltstone, are divided into the Obonai, Kunimitoge, Takinoue-onsen, and Yamatsuda Formations in order of decreasing age. The Kakkonda Granite, which has been encountered in the geothermal field at depths below 1140-2840m, has metamorphosed formations below the Kunimitoge Formation (Kato and Doi, 1993). WD-1a and WD-1b were drilled to intersect the western part of the Kakkonda Granite (Fig. 1).

The Kakkonda hydrothermal system consists of shallow deep reservoir, which are hydraulically connected. The shallow reservoir is permeable with a temperature of 230-260°C and is elongated in the NW-SE direction (Fig. 1). The deep reservoir has a temperature of 350-380°C. The boundary between the two reservoirs is around 1500m. The shallow reservoir is one to two orders of magnitude more permeable than the deep reservoir (Hanano, 1998). The heat conduction zone which is overlain by the deep reservoir at depth of ~3100m in the Kakkonda Granite in WD-1a has a temperature of over 380°C. (Ikeuchi et al., 1998).

Permeable fractures around WD-1 in the shallow reservoir strike northerly and dip at low angles (Kato et al., 1998). In the deep reservoir, permeable fractures are located mainly within and at the margin of the Kakkonda Granite. Seven deep wells have encountered the Kakkonda Granite. In five wells of these wells, the lost circulation (LC) occurred within twenty meters of the margin of the Kakkonda Granite (Kato et al., 1999).

3. FRACTURE OBSERVATIONS FROM SPOT CORES

Fourteen ~3m spot cores were retrieved from WD-1. Cores No. 4, 5 and 11 were oriented during drilling. The other eleven cores were not oriented during drilling, but orientations have been assigned to nine of these utilizing remanent magnetization, shape of core discing, and dip directions of bedding planes (Kato et al., 1998).

3.1 Fracture Distribution and Orientations

One feature of the shallow zone is a concentration of high-angle fractures striking NE to E. Other fractures in this shallow zone strike N to NW and E. Many veins from the cores No. 1-4 strike N to NW, and some drusy veins strike NW. Many slickensides striking NW are present in cores No. 1 and 3, and formed as a result of folding, since these dips parallel the bedding planes in the shale (Kato et al., 1998). The core observation indicates that the open fractures in the core No. 3 are the tension crack formed by the folding.

In the deep reservoir, many fractures observed in the core also strike NE to E. Core No. 11, collected from the deepest part of the deep reservoir within the Kakkonda Granite, has only two fractures, which lack obvious hydrothermal minerals. The fracture density in core of the Kakkonda Granite is far less than that seen in cores of the Miocene and pre-Tertiary formations (Fig. 2).

3.2 Permeable Fractures and Quartz Oxygen Isotopes

There are three types of quartz in the Kakkonda geothermal

field; a rock crystal, vein quartz, and fragment quartz. The rock crystals are formed in open fractures and druses around LC depths in the Kakkonda geothermal field. The existence of the rock crystal suggests the distribution of permeable fracture. The oxygen isotope ratio ($\delta^{18}O$) of liquid equilibrated with the rock crystals is lower than that with quartz from filled veins (Table 1). The $\delta^{18}O$ value of hot water in the shallow and deep reservoir ranges from –10.3 to -7.7 in $‰_{SMOW}$. This shows that the rock crystal is precipitated from the present and/or recent hot water, and the fracture with rock crystals is very young and permeable. Permeable fractures in the shallow and deep reservoirs belong to the N and E-trending fracture systems (Kato et al., 1998).

4. FRACTURES INTERPRETATED FROM FMI IMAGES

Through detailed analysis of FMI logs from WD-1a, we have been able to identify seven groups of planar structures: bedding, conductive fractures; closed fractures, faults, the intrusion boundary, drilling-induced tensile fractures (DTF), and others (Kato et al., 1998). We have divided fractures in WD-1b into conductive fractures and closed fractures from the FMI image (Fig. 3). Conductive fractures appear as thin conductive sine waves on these images. Closed fractures filled with highly resistive minerals (e.g. quartz or anhydrite) appear as thin, high-resistivity sine waves.

4.1 Fracture Density and Orientations

The interpreted fracture density of the FMI image in the Kunimitoge Formation is as high as 40-60 fractures/10m below ~2000m (Fig. 2). The fracture density from the FMI log is less than that of core observation, because the resolution of the FMI sonde is not as good as visual core observations. In the Obonai Formation, conductive fractures have three orientations; striking N0°E to N50°E and dipping 10-45°SE, and striking N10°W to N50°W and dipping 10-45°NE, and striking N20°E to N80°E and dipping 60-90°NW. The fracture density at the Obonai Formation is as high as 40-70 fractures/10m.

In the pre-Tertiary formations, conductive fractures strike N10°E to N90°E and dip 5-45°SE. These fractures are characteristic of low dip angle. The conductive fractures dipping at higher angles strike NW and NE. The fracture density is as high as 20-40 fractures/10m, and is different between sandy slate and slate. The sandy slate has more fractures than the slate.

In the Kakkonda Granite, the conductive fractures strike mainly NE and dip 20-50°SE. The conductive fractures dipping at higher angles strike ENE. The fracture density is mostly less than 10 fractures/10m, but the fracture density at the margin of the Kakkonda Granite is 24 fractures/10m. It shows that the margin of the Kakkonda Granite is permeable.

The number of conductive fractures and closed fractures is different in each formation. This was also seen in the spot cores. Differences in the fracture density and distribution between the Kakkonda Granite and the other formations may reflect the young age of the Kakkonda Granite and high temperature in the Kakkonda Granite.

4.2 Permeable Fracture Apertures and Orientations

Permeable fractures from FMI images are determined by the depth of lost circulation, and temperature and spinner logs. The permeable fractures in the Kunimitoge Formation strike in various directions and dip lower angles (Fig. 4). The permeable fractures in the Obonai Formation mainly strike N20°E to N35°E and dip 26-42°SE. In pre-Tertiary formations, the permeable fractures dip at high angles. These strike N8°E to N21°E and dip 70-82°NW, and strike N44°W and dip 54°SW. The permeable fractures in these formations have widths of 5-25 cm in conductive part on the FMI image. Fracture aperture in the core observations of the WD-1 cores is thinner than 5 mm.

In the Kakkonda Granite, most of the permeable fractures strike mainly NE and dip 28-89°SE. They have widths of 0.5-10 cm (mostly 0.5-5 cm) in conductive part of the FMI image. Although the number of the fractures is less in the Kakkonda Granite than in the pre-Tertiary formations, the permeability is greater than that in the pre-Tertiary formations (Fig. 2). The number of permeable fracture is apparently independent of fracture density.

5. STRESS ORIENTATION

5.1 Surface Observations

The fracture and vein orientations on the ground surface show the stress field at the time of fracture formation. $\sigma1$ of the principal stresses, ($|\sigma1|>|\sigma2|>|\sigma3|$) strikes NE and dips approximately horizontal. One vein belonging to the NE to E-trending fracture system contains K-feldspar, which yielded a K-Ar age of 0.2±0.1 Ma (Koshiya et al., 1993).

5.2 Core Observations

Cores No.3 and 4 have slickensides with striations and conjugate faults. The stress orientation is inferred by measurements of faults in the spot cores (Fig. 5). When the shear sense is unknown, there are two possible stress orientations, case 1 and case 2 in Fig 5b. The analysis by the shear sense and conjugate set indicates that the stress field at the time of fracture formation of core No.3 is normal fault type, and that of core no.4 is reverse-fault type. It shows these fractures were formed at different ages under different stresses.

5.3 Stress Orientations from the FMI Image

Through complex analysis of DTF shown on the FMI images in WD-1, we determined the principal stresses, around the well WD-1 using the method of Okabe et al. (1998). The principal stresses are as follows: at depths of 700-1300m, $\sigma1$ strikes W and is horizontal, $\sigma2$ dips vertically, and $\sigma3$ strikes northerly and is horizontal (Fig. 6). At depths of 1900-2650m around WD-1a, $\sigma1$ strikes WNW and dips ~60°, $\sigma2$ is oriented NE and horizontal, and $\sigma3$ strikes SE and dips ~20°. On the other hand, at depths of 2600-2910m around WD-1b, $\sigma1$ strikes WSW and is horizontal, $\sigma2$ is oriented SSE and is horizontal, and $\sigma3$ dips vertical. Therefor the stress field shows considerable variation with depth.

5.4 Focal Mechanisms of Micro-earthquakes

Temporal observations of micro-earthquakes were conducted between July 30 and November 22 1998. The fifteen temporal seismic stations were installed beside the ten permanent stations. Using initial motions of primary waves at these twenty-five stations, focal mechanism solutions of micro-

earthquakes were determined. We utilized the Micro-Earthquake data Processing and Analysis System (MEPAS) developed by Miyazaki et al. (1995).

Figure 7 shows the distribution of hypocenters with their focal mechanism solutions in the northwest part of the Kakkonda geothermal field. These focal mechanism solutions are plotted with equal area, upper hemisphere projection. Open circles are hypocenters whose focal mechanism solutions could not be determined. There are all types of focal mechanism solutions, strike-slip faults, reverse faults and normal faults. It shows two possibilities of faulting and stress state. One is that some micro-earthquakes occur along some existing faults. The other is that the stress state varies over small regions. It is likely that the latter is true, because some limited regions have similar focal mechanism solutions. The focal mechanism solution near WD-1 is strike-slip faulting (Fig. 7).

An analysis of micro-earthquakes ~1200m southeast from WD-1 (Fig. 1), at about 1500m depth, reveals that the corresponding $\sigma 1$ direction is ENE (Sugihara and Tosha, 1988). These researchers infer a fracture system involving both strike-slip and reverse faulting.

6. DISCUSSION

6.1 Distribution of Permeable Fractures

There is no difference in the fracture density in the Kunimitoge Formation whether it is in the shallow or deep reservoirs. The shallow reservoir has more open fractures than the deep reservoir. This shows that the permeable zone corresponds with the distribution of the open fractures and is independent of the fracture density.

6.2 Relation between Permeable Fractures and In Situ Stress

Most permeable fractures in the Kunimitoge Formation of shallow reservoir strike northerly and dip 10-40° E and W (Kato et al., 1998). The strike of these fractures is similar to the fold axes in the shallow reservoir (Fig. 1). The core observation of No. 3 and 4 indicates that the fractures striking northerly and dipping at low angles have been formed by reverse faulting and open fractures striking NNW have been formed by folding. Sugihara and Tosha (1988) infer a fracture system involving both strike-slip and reverse faulting at the present time. The stress state in the shallow reservoir around the WD-1 indicates strike-slip faulting, but there are few permeable fractures striking easterly and dipping at a high angle. These suggest that the permeable fractures are not necessarily formed by in-situ stresses at the present time and some permeable fractures are relatively old, opening and/or re-opening in-situ stress at present.

Tertiary and pre-Tertiary formations in the deep reservoir, the fractures have been formed by the same genesis at that of shallow reservoir. The contact metamorphism by the Kakkonda Granite caused the difference of the ratio of permeable fracture between shallow and deep reservoir.

The stress state around WD-1b indicates reverse faulting (Fig. 6c), but the FMI interpretation does not provide the genesis of permeable fracture formation in the Kakkonda Granite. The temperature and fracture distribution in the Kakkonda Granite indicates the idea of permeable fracture genesis. The Kakkonda Granite has been scarcely fractured by reverse faulting stress orientation, because the high temperature over 380°C is ductile condition of the granite. Fractures in the Kakkonda Granite have been probably formed by the cooling of the granite body after emplacement. Many fractures dip to the center of the Kakkonda Granite like cooling joints of the intrusive rocks (Fig. 4). After that, these joints are critically stressed at the present time and opening and/or re-opening.

7. CONCLUSIONS

The Kakkonda geothermal field has many fractures with various strikes and dips. These fractures have been formed recently and some time ago. The $\delta^{18}O$ value of the rock crystals within veins indicates whether the fracture is permeable or not. The permeable zone corresponds with the distribution of the open fractures independently of the fracture density. The permeable fractures are not necessarily formed in in-situ stress conditions at the present time. The folding of the Tertiary formation and the cooling of the Kakkonda Granite are important for permeable fracture genesis. Permeable fractures formed some time ago keep opening and/or re-open under present stress conditions.

ACKNOWLEDGMENTS

The authors wish to thank Takashi Akatsuka and Satoshi Takemoto of JMC Geothermal Engineering Co., Ltd. (Geo-E) for their help in collecting the fracture data. They also thank Naoko Yano and Seiko Yokokawa for processing of micro-earthquake data by MEPAS, and NEDO and JMC for their permission to publish this paper.

REFERENCES

Doi, N., Kato, O., Ikeuchi, K., Komatsu, R., Miyazaki, S., Akaku, K. and Uchida, T. (1998). Genesis of the plutonic-hydrothermal system around Quaternary granite in the Kakkonda geothermal system, Japan, *Geothermics,* Vol.27, pp.663-690.

Hanano, M. (1998). A simple model of a two-layered high-temperature liquid-dominated geothermal reservoir as a part of a large-scale hydrothermal convection system, *Transport in Porous Media*, Vol.33, pp.3-27.

Ikeuchi, K., Doi, N., Sakagawa, Y., Kamenosono, H. and Uchida, T. (1998), High-temperature measurements in well WD-1a and the thermal structure of the Kakkonda geothermal system, Japan, *Geothermics*, Vol.27, pp.591-607.

Kato, O. and Doi, N. (1993). Neo-granitic pluton and later hydrothermal alteration at the Kakkonda geothermal field, Japan. *Proceedings 15th NZ Geothermal Workshop*, pp.155-161.

Kato, O., Doi, N., Sakagawa, Y. and Uchida, T. (1998). Fracture systematics in and around well WD-1, Kakkonda geothermal field, Japan, *Geothermics*, Vol.27, pp.609-629.

Kato,O., Sakagawa,Y., Doi,N., Akaku,K. and and Ohkubo,Y. (1999). Permeable fractures in the Kakkonda Granite of well WD-1b, Japan. *Proceedings 24th Workshop on Geothermal Reservoir Engineering, Stanford University, submitted to Stanford University*, pp.243-249.

Koshiya, S., Okami, K., Kikuchi, Y., Hirayama, T., Hayasaka, Y., Uzawa, M., Honma, K. and Doi, N. (1993). Fracture

system developed in the Takinoue geothermal area. *Jnl. Geothermal Research Society Japan*, Vol.15, pp.109-139. In Japanese with English abstract.

Matsuhisa,Y., Goldsmith,J.R. and Clayton,R.N. (1979). Oxygen Isotopic Fractionation in the System Quartz-Albite-Anorthite-Water. *Geochim. Cosmochim. Acta*, Vol.43, p.1131-1140.

Miyazaki, S., Hanano, M., Kondoh, T., Yoshizawa, H., Kajiwara, T., Tsuchibuchi, S., Takahashi, M., Muraoka, H., Nagano, S. and Mitsuzuka, T. (1995). Micro-earthquakes data processing and analysis system (MEPAS), a software for geothermal applications, *Proc. WGC 1995, Florence, Italy*, pp.3023-3028.

Okabe,T., Hayashi,K., Shinahara,N. and Takasugi,S. (1998). Inversion of drilling-induced tensile fracture data obtained from a single inclined borehole. *Int. Jnl. Rock Mech. Min. Sci. & Geomech. Abstr.*, Vol.35, pp.747-758.

Sugihara, M. and Tosha, T. (1988). A microearthquake study of the fracture structure in the Takinoue geothermal area. In: *Proc. Internat. Symp. Geothermal Energy. 1988. Kumamoto and Beppu, Japan*, pp.105-108.

Table 1. Oxygen isotope ratio of quartz

Well name	Depth (m)	Sample	$\delta^{18}O_{QZ}$	Temperature (℃)	$\delta^{18}O_{HW}$
WD-1	50m	Vein Quartz and Fragment Quartz	+8.3	235	-1.3
WD-1	155.90m	Rock Crystal	+3.6	182	-9.2
WD-1	960m	Rock Crystal and Fragment Quartz	+8.0	240	-1.4
WD-1	1,220.85m	Vein Quartz	+5.5	252	-3.3
WD-1	1,221.00m	Vein Quartz	+6.7	252	-2.1
WD-1	1,447.35m	Rock Crystal	-3.1	312	-9.5
WD-1	1,695.95m	Vein Quartz	+7.1	338	+1.5
WD-1a	1,942.5m	Rock Crystal	-3.6	350	-8.9
WD-1a	2,276.20m	Vein Quartz	+5.9	353	+0.7
WD-1b	2,475m	Rock Crystaland Vein Quartz	-3.6	368	-8.4
WD-1b	2,820.15m	Vein Quartz	+6.5	382	+2.0
WD-1a	3,230.05m	Vein Quartz	-3.1	410	-6.9
WD-1a	3,728.10m	Vein Quartz	+8.3	519	+6.3

Temperature : Average of homogenization temperature of fluid includion
$\delta^{18}O_{QZ}$: oxygen isotope ratio of quartz in ‰SMOW
$\delta^{18}O_{HW}$: oxygen isotope ratio of water in ‰SMOW calcurated by the method of Matsuhisa et al.(1979)

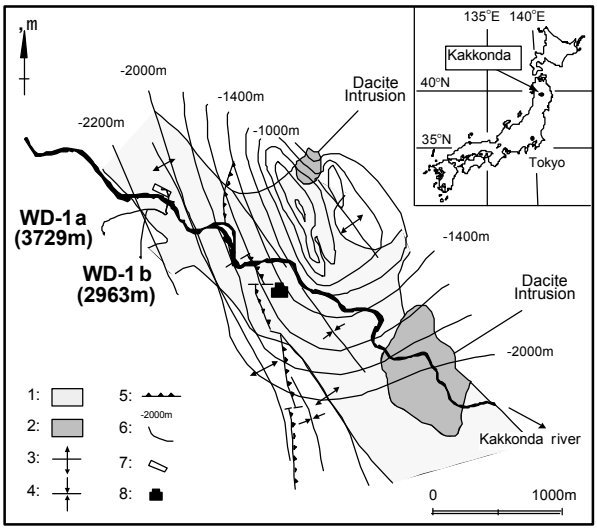

Figure 1. Generalized geology of the Kakkonda geothermal field showing well locations (Kato et al., 1998). 1: Permeable zone in the shallow reservoir, 2: dacite intrusion, 3: anticlinal axis, 4: synclinal axis, 5: fault (ornaments on downthrown block), 6: contour of the top of the Kakkonda Granite (relative to sea level), 7: drill pad, 8: power plants.

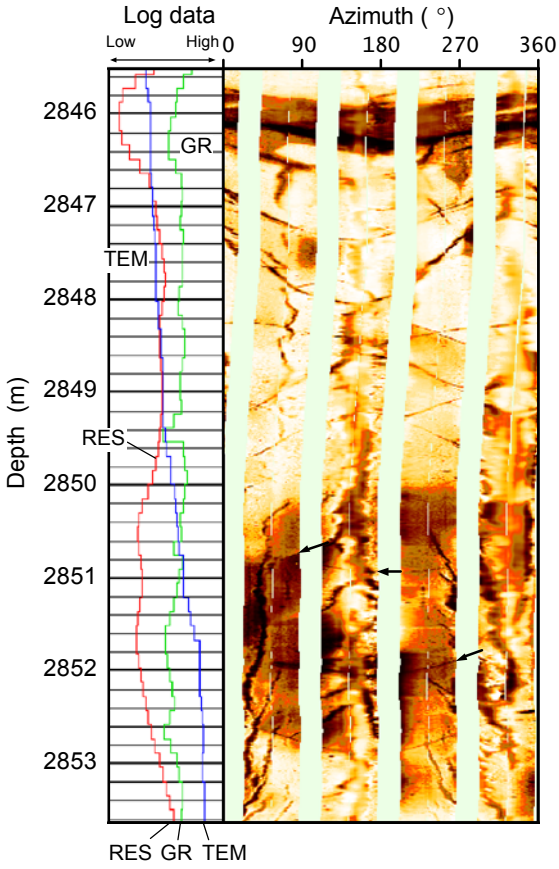

Figure 3. The FMI image and the log data in the permeable zone in the Kakkonda Granite from well WD-1b (Kato et al., 1998). Arrows show permeable fractures between 2850 and 2852m. Bright color indicates high resistivity, dark color indicates low resistivity in the image. RES; Resistivity, GR; Gamma ray. TEM; Temperature while injecting water .

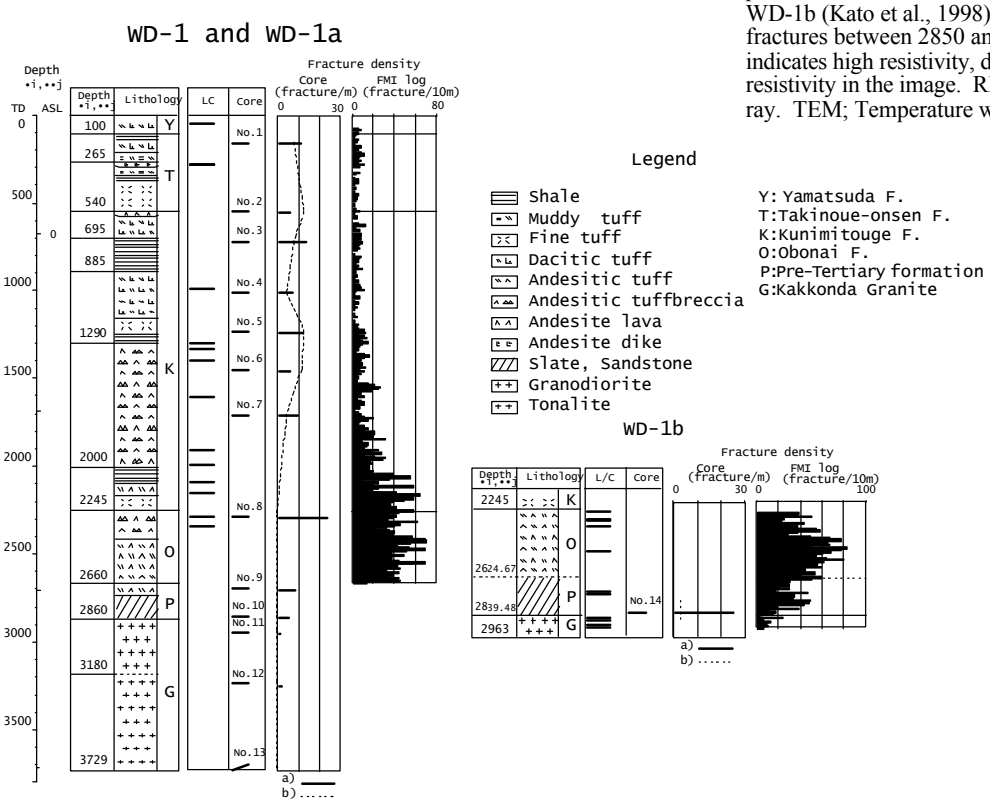

Figure 2. Compiled column of WD-1. LC: lost-circulation depth, Core: the number of the spot core, Fracture density: the result of core observation and inerpretation from the Schlumberger's FMI log, a) fracture density, b) the ratio of open fracture from all fractures at the core in %.

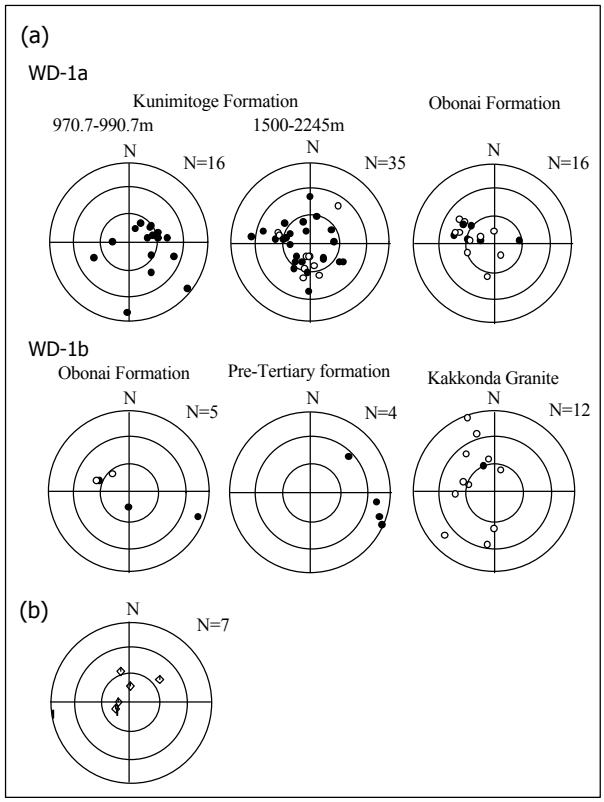

Figure 4. π-pole diagrams of permeable fractures from FMI logs and core observations. Equal-area, lower-hemisphere projection. a) Permeable fracture from FMI data, open circle; apparent width of low resistivity in FMI image is from 5 mm to 10 cm, solid circle; apparent width of low resistivity in FMI image is over 10 cm. b) Permeable fractures from cores No.3, 4, 5 and 7.

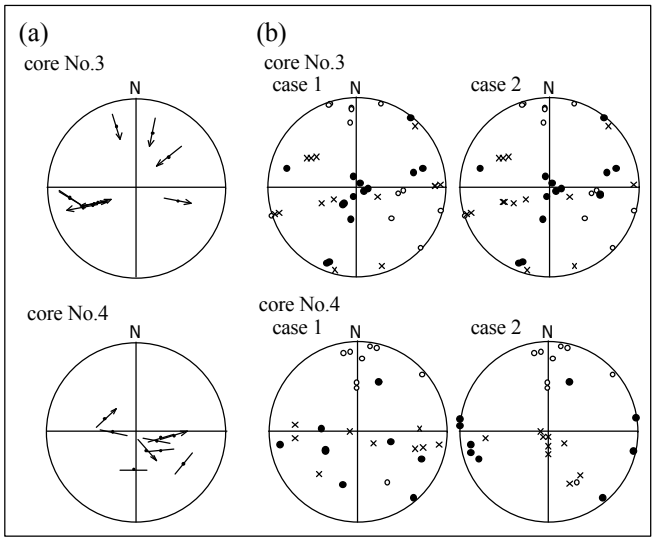

Figure 5. (a) Fault populations of in WD-1 from cores No.3 and 4. Poles of slickensides with traces. The arrow indicates the shear sense of the hanging wall. (b) Orientation of principal stress axes from fracture analysis. Lower hemisphere plots. Solid circle; maximum principal stress axis. Open circle; intermediate principal stress axis. Cross; minimum principal stress axis.

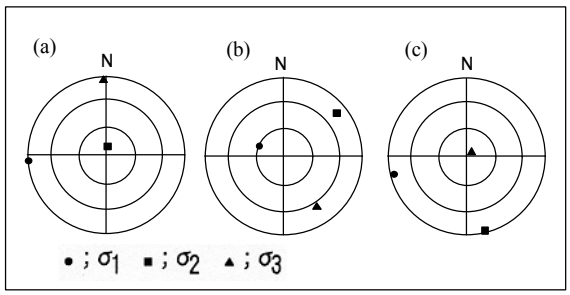

Figure 6. In situ stress orientation. (a) Shallow reservoir, 700-1300m in WD-1. (b) Deep reservoir, 190 0-2650m in WD-1a. (c) Deep reservoir, 2600-2910m in WD-1b.

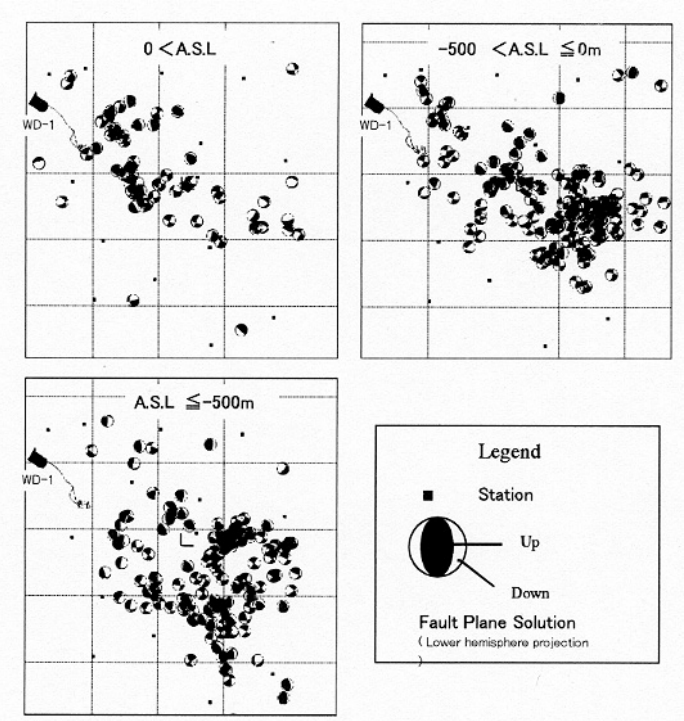

Figure 7. The distribution of hypocenters with their focal mechanism solutions in the northwest part of the Kakkonda geothermal field.